AFRL-AFOSR-UK-TR-2022-0027

Development of High- Brightness Continuous-Wave Mid-Infrared Quantum-Cascade Laser

Masselink, William
Humboldt-Universitat zu Berlin
Unter den Linden 6
Berlin, , 10099
DE

03/09/2022
Final Technical Report

Air Force Research Laboratory
Air Force Office of Scientific Research
European Office of Aerospace Research and Development
Unit 4515 Box 14, APO AE 09421

REPORT DOCUMENTATION PAGE

PLEASE DO NOT RETURN YOUR FORM TO THE ABOVE ORGANIZATION.

1. REPORT DATE	2. REPORT TYPE	3. DATES COVERED	
20220309	Final	START DATE 20180930	END DATE 20210929

4. TITLE AND SUBTITLE
Development of High- Brightness Continuous-Wave Mid-Infrared Quantum-Cascade Laser

5a. CONTRACT NUMBER	5b. GRANT NUMBER	5c. PROGRAM ELEMENT NUMBER
	FA9550-18-1-7020	61102F
5d. PROJECT NUMBER	**5e. TASK NUMBER**	**5f. WORK UNIT NUMBER**

6. AUTHOR(S)
William Masselink

7. PERFORMING ORGANIZATION NAME(S) AND ADDRESS(ES)
Humboldt-Universitat zu Berlin
Unter den Linden 6
Berlin 10099
DE

8. PERFORMING ORGANIZATION REPORT NUMBER

9. SPONSORING/MONITORING AGENCY NAME(S) AND ADDRESS(ES)	10. SPONSOR/MONITOR'S ACRONYM(S)	11. SPONSOR/MONITOR'S REPORT NUMBER(S)
EOARD UNIT 4515 APO AE 09421-4515	AFRL/AFOSR IOE	AFRL-AFOSR-UK-TR-2022-0027

12. DISTRIBUTION/AVAILABILITY STATEMENT
A Distribution Unlimited: PB Public Release

13. SUPPLEMENTARY NOTES

14. ABSTRACT
Project progress was significantly delayed due to partial lockdown in 2020 related to covid-19. The resulting delay required further work into the beginning of 2022 (during the cost-neutral project prolongation) to complete the planned tasks. All the tasks and milestones have been thus fully completed. The project has resulted in fabrication of numerous Quantum Cascade Laser (QCL) wafers and an actual operating devices; in development of highly-efficient broad-gain design with power conversion efficiency above 6% in a number of low-threshold designs for the targeted spectral range of 8-to-9.5 Î¼m; and in the demonstration of a reliable mode restriction to the single TM00 in the broad-area tapered waveguides with the taper widths up to 100 Î¼m (again supporting our theoretical predictions). The broad QCL-design and device-fabrication experience obtained in the project will be implemented within other current and future development projects.

15. SUBJECT TERMS

16. SECURITY CLASSIFICATION OF:			17. LIMITATION OF ABSTRACT	18. NUMBER OF PAGES
a. REPORT U	b. ABSTRACT U	c. THIS PAGE U	SAR	9

19a. NAME OF RESPONSIBLE PERSON	19b. PHONE NUMBER *(Include area code)*
NATHANIEL LOCKWOOD	314-235-6005

Development of High-Brightness Continuous-Wave Mid-Infrared Quantum-Cascade Laser

W. T. Masselink and M. P. Semtsiv
Humboldt University Berlin, Newtonstr. 15, 12489 Berlin, Germany

Project report for the year 2021

Summary

This document reports the results of USAF Grant FA9550-18-1-7020 during its third 12 months.
The objective for the third project period (year 2021) was high brightness emission within 8.5–9.0 µm.

This phase used the results of the previous time periods for guidance, but targeted this longer wavelength with several totally new structure designs.

QCL structures were epitaxially grown using gas-source molecular-beam epitaxy following a new paradigm of reduced cascade number, processed into BA bars using optical lithography combined with wet and dry etching, facet-coated for optimized power, mounted, and tested.

Within the above objective, the following four tasks were formulated for each project quarter:

Task 1: Design and first growths of QCL emitting at 8.5–9.0 µm. The task is fully executed. Twelve QCL designs were developed. Using these and several reference designs, 23 QCL structures were fabricated and characterized.

Task 2: Processing of first tapered QCLs. Demonstration of RT cw operation of the tapered QCL with the tapered facet ca. 50 µm. Demonstration of a single-lobe in the far field for the tapered QCL. The task is partially executed (the QCLs are processed, but cw operation is not achieved; the characterization of tapered waveguides will be complete soon and communicated separately).

Task 3: Optimization of the AR facet coating. Demonstration of the RT cw operation of tapered QCL with average power >0.3 W. The task is partially executed. We have advanced our facet-coating technique, but cw operation was not demonstrated.

Task 4: Optimization of the tapered waveguide shape. Demonstration of $M^2_x < 3$. The task is fully executed. The tapered waveguide design and fabrication for the wavelength range is fully developed. The far-field measurements show primarily fundamental mode with single lobe.

To summarize, the tasks were generally successfully completed. We have designed, grown, fabricated, and characterized a large number of long wavelength QCLs. We have achieved a number of good original QCL active region designs with low threshold current density. But, we were not able to demonstrate cw operation in the targeted spectral range, which is mainly due to the lack of wall-plug efficiency.

Project results

QCL designs:

According to the project work-plan we have designed a number of original QCL active regions. The table below summarizes the most-successful designs, which were later fabricated and characterized.

Design name	**Active region**	**Grown wafers**	**Highlights**
5QW-1	lattice-matched	0725	high dipole matrix element, z=4.73nm, design 9.5µm
5QW-2	lattice-matched	0726	high dipole matrix element, z=4.78nm, design 9.5µm
5QW-3	strain-compensated	0727	dipole matrix element z=3.50nm, design 8.1µm
6QW	strain-compensated	0728	dipole matrix element z=4.32nm, design 9.0µm
BG-1	strain-compensated	2178	broad gain, design ~9µm
BG-2	strain-compensated	2183	broad gain, design ~9µm
BG-3	strain-compensated	2184	broad gain, design ~9µm
BG-4	strain-compensated	2185	broad gain, design ~9µm
BG-5	strain-compensated	2186	broad gain, design ~9µm
BG-6	strain-compensated	2187	broad gain, design ~9µm
BG-7	strain-compensated	2188	broad gain, design ~9µm
HVE	strain-compensated	2521, 2523	high-voltage-efficiency, design ~8µm

We investigated three different categories of designs: In one category (HDM) (designs 5QW-1, 5QW-2, 5QW-3, and 6QW), the dipole matrix element, z, was maximized by using a large number of quantum wells in active region; in the second category (BG-1 through BG-7), the injection efficiency was maximized within a broad-gain type design; and in the third category (HVE), the voltage efficiency was optimized (i.e. the voltage defect reduced) by using just three quantum wells in the active region and a shallow injector band. The figures below illustrate the band alignment of the three designs, representing the three design categories.

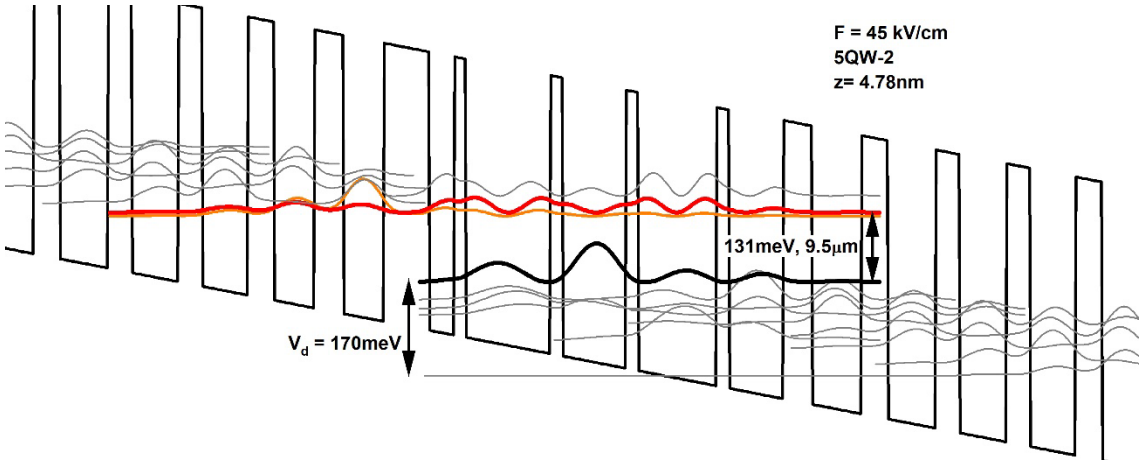

Fig. 1. Conduction band edge profile and the relevant Wannier-Stark states of a typical high-dipole-matrix (HDM) design, the 5QW-2 design (wafer 0726). Advantage of the 5 QWs design is the high dipole matrix element of the laser transition, which reduces the threshold current.

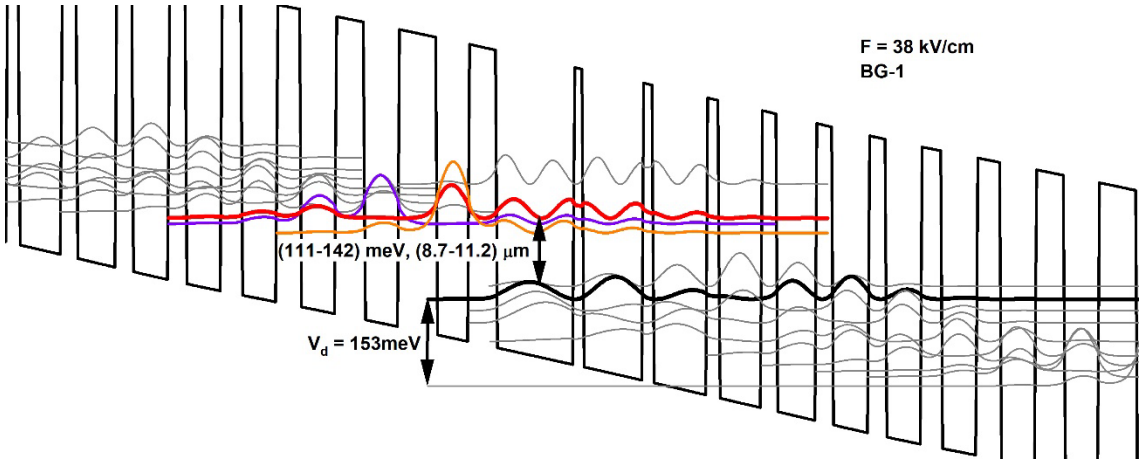

Fig. 2. Conduction band edge profile and the relevant Wannier-Stark states of the BG-1 design (wafer 2178). Advantage of the broad-gain design is the reduction of the interface-roughness scattering impact on the laser performance.

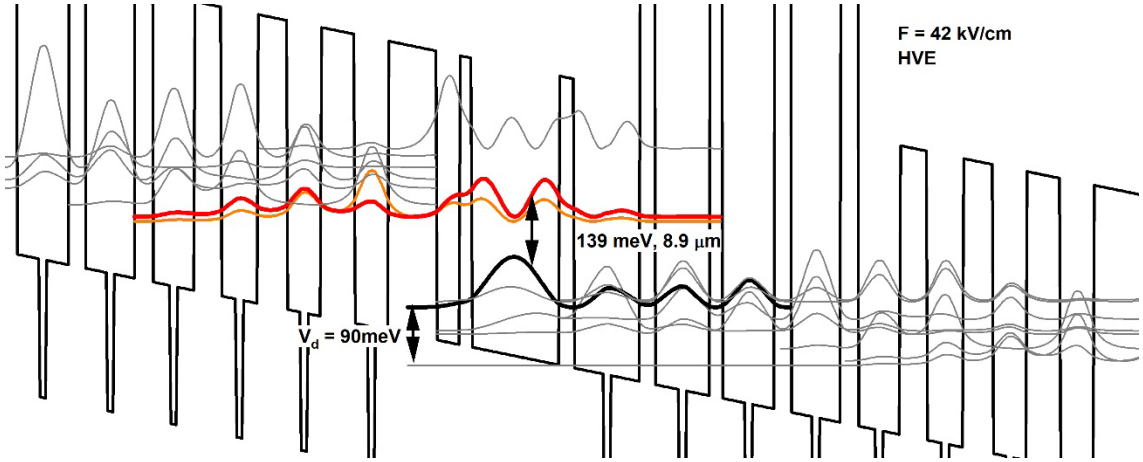

Fig. 3. Conduction band edge profile and the relevant Wannier-Stark states of the high-voltage-efficiency (HVE) design (wafer2521). Advantage of this design is the reduction of the so-called defect voltage V_d below 100 meV and increase of the upper-laser-state confinement by using of high AlAs barriers in the injector region.

QCL growth:

Altogether there has been 23 QCL wafers grown in the course of this third year with cascade number ranging between 10 and 100. These QCLs involve four literature designs of Refs. [Yu06, Green04, Wang09, Fujita11] and twelve original active region designs. The list of the grown QCL wafers is summarized in the table below.

Grown wafer	**Design**	**No. of cascades**	**Waveguide**	**Wavelength (μm)**	**J_{th} @RT (kA/cm2)**	**J_{max} @RT (kA/cm2)**
0722	Yu06	50	InGaAs/InP	10.6	2.6	7.3
0723	Green04	35	InP	10.8	4.5	-
0724	Yu06	35	InGaAs/InP	10.1	2.9	-
0725	5QW-1	35	InP	-	3.3	-
0726	5QW-2	35	InP	10.7	2.5	-
0727	5QW-3	35	InP	9.4	3.7	-
0728	6QW	35	InP	10.2	10.6	high doping
0729	Green04	20	InP	-	-	don't lase
0730	Green04	10	InP	-	-	don't lase
1828	Fujita11	40	InGaAs/InP	9.3—9.7	2.3	4.3
1900	Fujita11	100	InGaAs/InP	10.3	2.0	5.0
2003	Fujita11	40	InGaAs/InP	10.4—10.5	3	4.9
2004	Fujita11	40	InGaAs/InP	10.2—11.1	5	>12
2023	Fujita11	40	InGaAs/InP	10.5—10.6	2.2	3
2025	Fujita11	40	InGaAs/InP	10.8—11.3	2.2	5.1
2047	Fujita11	45	InGaAs/InP	10.2—11.1	-	-
2178	BG-1	100	InGaAs/InP	9.6—10.7	1.3	3.3
2183	BG-2	100	InGaAs/InP	8.9—9.6	2.5	5.3
2184	BG-3	100	InGaAs/InP	9.2—10.0	1.5	4.3
2185	BG-4	100	InGaAs/InP	8.5—9.2	2.0	-
2186	BG-5	100	InGaAs/InP	9.0—9.7	2.3	3.5
2187	BG-6	100	InGaAs/InP	8.9—10.3	-	-
2188	BG-7	100	InGaAs/InP	8.7—9.2	3	-
2521	HVE	40	InGaAs/InP	tbd	tbd	high doping

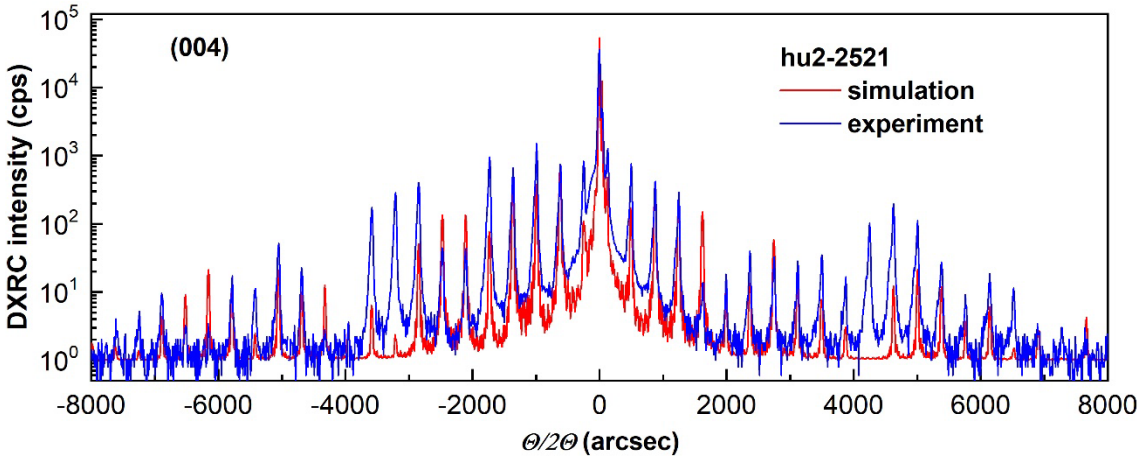

Fig. 4. Example of high-quality result of X-ray wafer characterization: measured (004) rocking curve of the strain-compensated QCL wafer hu2-2521 (blue) and theoretical simulation (red). Narrow peaks of the rocking curve satellites indicate high crystal quality.

Device fabrication and testing:

For the standard device characterization in pulsed mode, each wafer was processed in a conventional broad-area Fabry-Perot laser device using optical lithography and wet chemical etching. After fabrication the wafer was cleaved into laser bars of various lengths and tested, usually with 100-ns-long current pulses at 10 kHz repetition frequency. Laser spectra were measured using IFS-66 FTIR, usually with resolution of 1 cm^{-1}, except otherwise specified. Most of the QCLs hit the targeted spectral range (8-to-9.5 μm). The spectral width of the broad-gain designs was sometimes broader than the targeted spectral range, so these designs could not really fit within 8-to-9.5 μm. Figure 5 below illustrates this result.

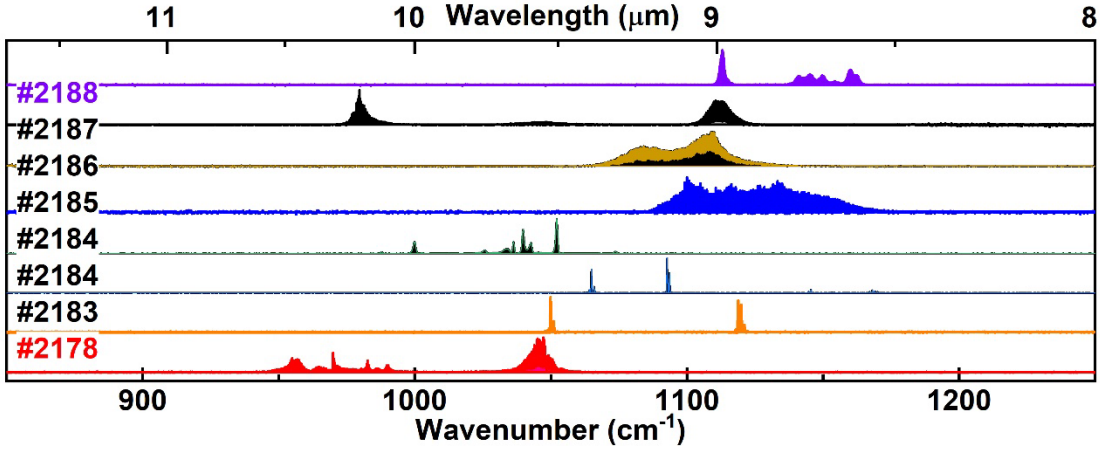

Fig. 5. QCL emission spectra of the group of strain-compensated broad-gain designs, measured in pulsed mode at room temperature. (wafer numbers are indicated). All of the lasers, except #2178, lased within the targeted spectral range of 8-to-9.5 μm.

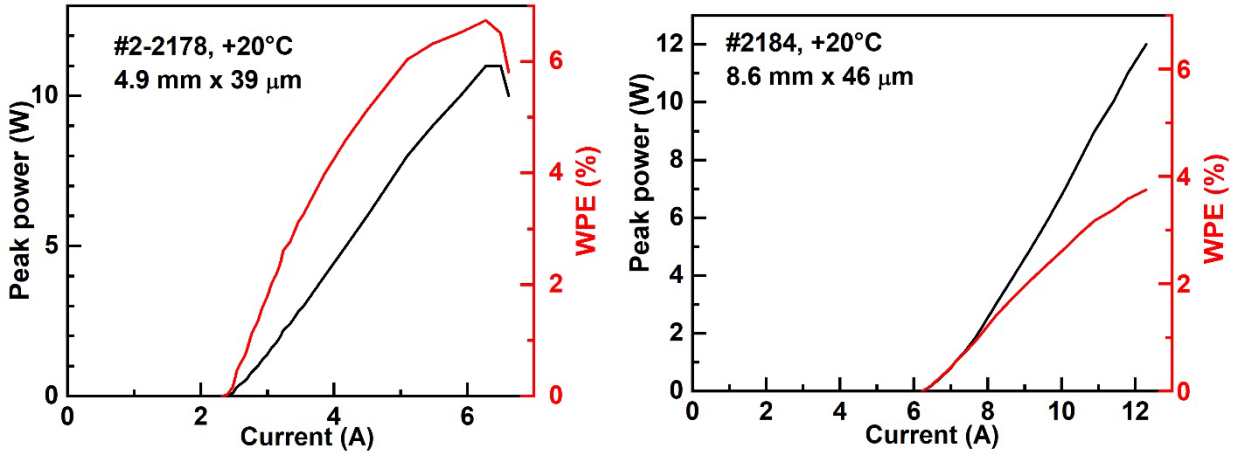

Fig. 6. Pulsed power and efficiency curves of the broad-area lasers made of the two strain-compensated broad-gain laser samples: wafer #2178, 4.9-mm-long and 39-μm-wide device and wafer #2184, 8.6-mm-long and 46-μm-wide device. Wafers #2178 and #2184 have shown the highest power conversion efficiencies >6% and maximum pulse power >10 W, in the current project period.

Buried-heterostructure waveguides:

Two selected wafers (#1828, #2004) were also processed into buried-heterostructure devices with an effort to demonstrate the continuous-wave (cw) operation. Figure 7 below plots the power efficiency for these two samples. The efficiency performance of the buried-heterostructure waveguides in the given coordinates almost coincides with the reference dielectric-isolated double-trench waveguide (left panel) and is almost the same for various waveguide widths (right panel). This result indicates that the leakage current and additional optical losses in the buried-heterostructure waveguide are negligible. Despite of the successful waveguide regrowth, room temperature cw operation was not achieved in these two structures. Apparently, the buried-heterostructure waveguide fabrication – known to be a very demanding technique – requires further improvements in our lab. Good preliminary results have been recently obtained by replacing the compensating Fe used in the re-grown InP with Rh and Ru. This and other improvements will be pursued in other current and future projects.

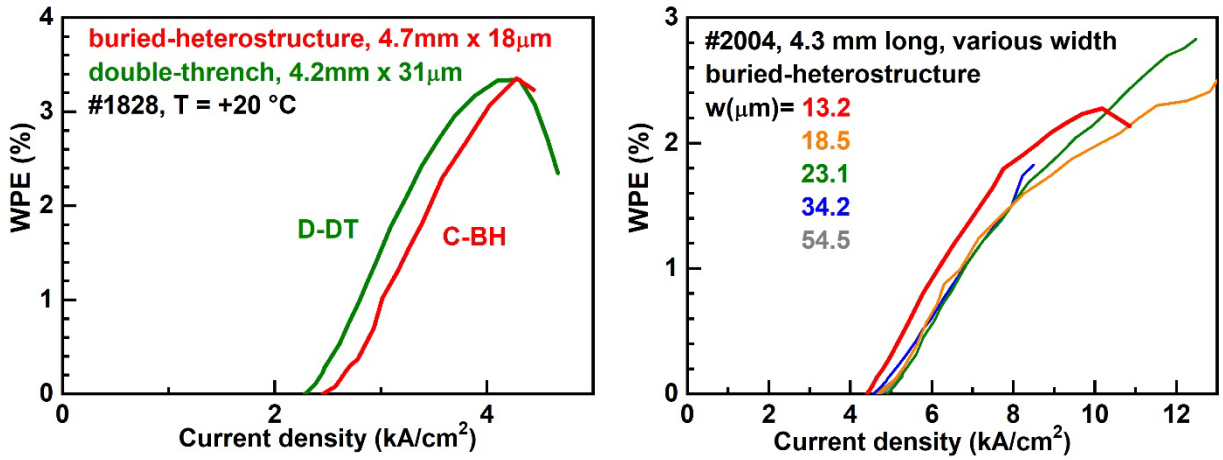

Fig. 7. Pulsed power efficiency curves of the broad-area lasers made of the two strain-compensated broad-gain laser samples: wafer #2178, 4.9-mm-long and 39-μm-wide device and wafer #2186, 4.0-mm-long and 45-μm-wide device.

Tapered waveguides:

A tapered waveguide design has been calculated and masks for its processing have been designed. Figure 8 below illustrates the choice of the taper parameters with two target taper designs.

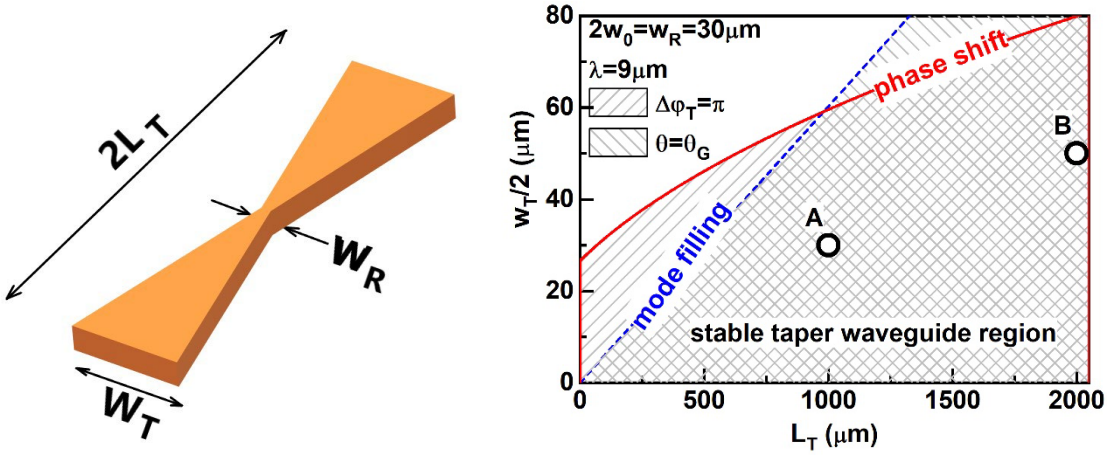

Fig. 8. Left: schematic illustration of the chosen tapered-waveguide design. Right: parameter space, illustrating the choice of the stable taper waveguide design (after Ref. [Semtsiv20]). Two open circles point the two chosen taper designs for the 9 μm emission wavelength (A: taper waist w_R= 30 μm, taper length, L_T= 1 mm, full taper width, w_T= 60 μm and B: taper waist w_R= 30 μm, taper length, L_T= 2 mm, full taper width, w_T= 100 μm).

The designed taper shapes A and B shown in Fig. 8 have been lithographically implemented for the wafer #2178 using a direct-laser-beam-writing instrument. The laser fabrication was then completed with our standard SiO_2 insulation of the laser ridge side-walls using reactive-gas magnetron sputtering, the top and the bottom Cr/Au metallization by thermal evaporation, and the top contact enforcement by galvanic gold deposition. The 4-mm-long tapered laser bars of both designs were cleaved through the taper point as illustrated on the inserts of the two sides of Fig. 9 below. On the 4-mm-long bars we fit exactly two patterns of design A or just one pattern of design B. Measuring both tapered laser shapes with the same total length is appropriate for direct comparison, since the facet losses must be the same in this case. Both tapered waveguides (A with 60-µm-wide taper and B with 100-µm-wide taper) support a pure fundamental mode, as demonstrated with the beam cross-sections at the figures below measured at 6 mm distance from the facet.

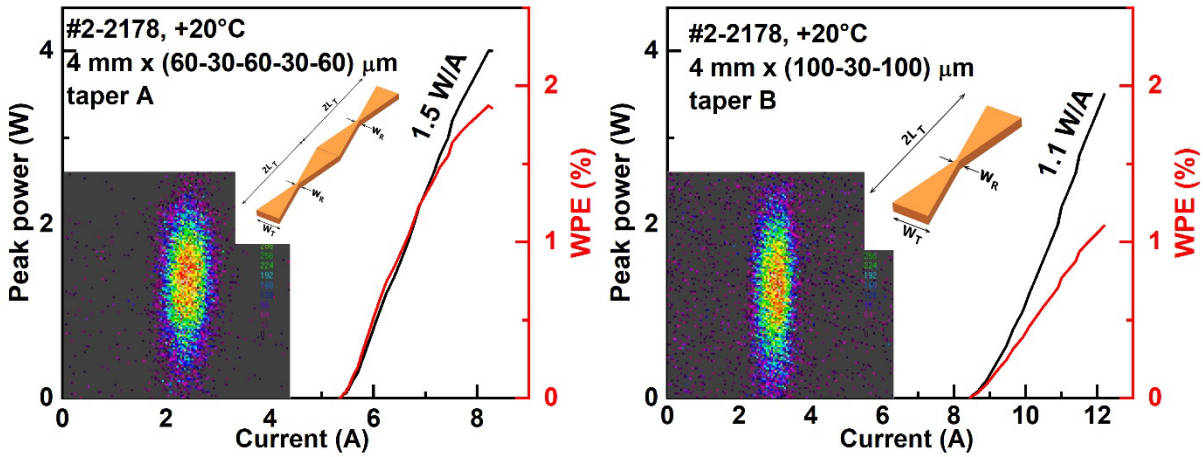

Fig. 9. Pulsed power and efficiency curves of the broad-area tapered lasers made of the wafer #2178. Left panel shows the performance of the 4-mm-long section of the taper design A with taper waist w_R= 30 µm, taper length, L_T= 1 mm, full taper width, w_T= 60 µm as illustrated on the insert. Right panel shows the performance of the 4-mm-long section of the taper design B with taper waist w_R= 30 µm, taper length, L_T= 2 mm, full taper width, w_T= 100 µm as illustrated on the insert. Both, the 60-µm-wide and the 100-µm-wide, tapered waveguides support exclusively the fundamental mode as shown by the inserted beam cross-sections measured at 6 mm distance from facet at the pulse current of 7 A (taper A, left) and 10 A (taper B, right).

Conclusions and outlook

Project progress was significantly delayed due to partial lockdown in 2020 related to covid-19. The resulting delay required further work into the beginning of 2022 (during the cost-neutral project prolongation) to complete the planned tasks. All the tasks and milestones have been thus fully completed. The project has resulted in fabrication of numerous QCL wafers and operating devices; in development of highly-efficient broad-gain design with power conversion efficiency above 6% in a number of low-threshold designs for the targeted spectral range of 8-to-9.5 µm; and in the demonstration of a reliable mode restriction to the single TM_{00} in the broad-area tapered waveguides with the taper widths up to 100 µm (again supporting our theoretical predictions). The broad QCL-design and device-fabrication experience obtained in the project will be implemented within other current and future development projects.

References

[Yu06] High-power 9.5 μm quantum-cascade lasers operating above room temperature in continuous-wave mode, J. S. Yu, S. Slivken, A. Evans, S. R. Darvish, J. Nguyen, and M. Razeghi, Appl. Phys. Lett. **88**, 091113 (2006).

[Green04] High-performance distributed feedback quantum cascade lasers grown by metalorganic vapor phase epitaxy, R. P. Green, L. R. Wilson, E. A. Zibik, D. G. Revin, J. W. Cockburn, C. Pflügl, W. Schrenk, G. Strasser, A. B. Krysa, J. S. Roberts, C. M. Tey, and A. G. Cullis, Appl. Phys. Lett. **85**, 5529 (2004).

[Wang09] High performance quantum cascade lasers based on three-phonon resonance design, Q.J. Wang, C. Pflügl, L. Diehl, F. Capasso, T. Edamura, S. Furuta, M. Yamanishi, and H. Kan, Appl. Phys. Lett. **94**, 011103 (2009).

[Fujita11] Broad-gain ($\Delta\lambda/\lambda 0 \sim 0.4$), temperature-insensitive ($T0 \sim 510K$) quantum cascade lasers, K. Fujita, S. Furuta, T. Dougakiuchi, A. Sugiyama, T. Edamura, and M. Yamanishi, Opt. Express **19**, 2694 (2011).

[Semtsiv20] Fundamental mode emission in tapered quantum cascade lasers for high brightness, M. P. Semtsiv and W. T. Masselink, Optical Engineering **59**, 086101 (2020); https://doi.org/10.1117/1.OE.59.8.086101.